# Use HF Signal Injection for Simultaneous Rotor Angle, Torque and Temperature Estimation in PMSMs

Marcos Orviz Zapico
University of Oviedo. Dept of Elect. Computer & System Engineering, Gijón, 33204, Spain
orvizmarcos@uniovi.es

David Díaz Reigosa
University of Oviedo. Dept of Elect. Computer & System Engineering, Gijón, 33204, Spain
diazdavid@uniovi.es

Diego Fernández Laborda
University of Oviedo. Dept of Elect. Computer & System Engineering, Gijón, 33204, Spain
dflaborda@uniovi.es

María Martínez Gómez
University of Oviedo. Dept of Elect. Computer & System Engineering, Gijón, 33204, Spain
martinezgmaria@uniovi.es

Juan Manuel Guerrero Muñoz
University of Oviedo. Dept of Elect. Computer & System Engineering, Gijón, 33204, Spain
guerrero@uniovi.es

Fernando Briz del Blanco
University of Oviedo. Dept of Elect. Computer & System Engineering, Gijón, 33204, Spain
fernando@isa.uniovi.es

***Abstract*— Use of high frequency (HF) signal injection-based methods with PMSMs has been widely investigated for several purposes including rotor angle/speed estimation, permanent magnet (PM) temperature estimation and torque estimation. This paper analyses the opportunities of multi-estimation. The physics behind these methods are analyzed, from which the number and characteristics of the HF signals to be injected can be deduced. Based on this, injection of a pulsating HF current 45º shifted from the *d*- axis and a rotating HF current in the stationary reference frame is found to be a suitable solution for simultaneous rotor angle, torque and magnet temperature estimation.**[1]

***Keywords*— Permanent Magnet Synchronous Machine (PMSM), high frequency signal injection, sensorless control, torque estimation, temperature estimation***

## I. Introduction

The use of PMSMs has increased during the last decades in a large variety of applications thanks to their improved performance in terms of torque/power density, efficiency, and controllability compared to other types of electric machines. Torque and motion control of PMSMs drives requires knowledge of the rotor angle, which can be measured or estimated. In addition, knowledge of machine torque and magnet temperature can be highly desirable for control and reliability purposes.

Optical encoders and resolvers, are the preferred solution in the industry for rotor angle feedback [1]-[2] , though other alternatives are available [3]-[5]. Cost of the position sensor and the associated cabling and interfaces can account for a significant portion of the overall drive cost, especially in low-power applications. In addition, the sensor itself and the associated cabling and connectors can be a source of failures, reducing the drive reliability. Elimination of the position/speed sensor is therefore desirable. Sensorless methods are an alternative to the use of position sensors [6]-[20]. Sensorless methods can be broadly classified into methods based on the fundamental excitation [6], and saliency tracking based techniques [7]-[20].

Fundamental excitation-based methods are effective when the back electromotive force (BEMF) signal is sufficiently large, i.e., at medium and high speeds; operation at low speed or standstill not being possible. Saliency tracking based techniques were proposed to overcome the limitations of BEMF based methods in the low-speed range, since they allow rotor angle estimation at low and zero speed.

Precise knowledge of the torque produced by the machine is also a highly appealing feature in many applications [21]. Torque measurement can be done using strain gauges [22], other methods like those based on torsional displacements being less extended [23]. Independently of the method, torque measurement is costly and requires additional cabling and room. Hence, torque estimation is preferred in most applications. Torque estimation methods include equation based methods [24]-[28], indirect estimation methods [29] and neural networks [30]. All these methods require knowledge of certain machine parameters (e.g., magnet flux, inductances, and resistances) which often can vary with machine operating conditions (e.g., temperature, saturation, or speed). Injection of a HF signal into the stator terminals of the machine has been reported as a viable option for real time adaption of machine parameters needed by torque estimation methods, eventually enhancing their accuracy [27].

Finally, the performance and reliability of the drive also depends on the PMSM temperature, especially PMs' temperature. Magnet temperature can be measured by means of contact type sensors (e.g., PTC thermistors, thermocouples, etc.) or non-contact type sensors (e.g., IR sensors) [31]. However, PM temperature measurement is not easy in practice as it implies modifications of the machine design, which can affect to its

Table I. Estimation information from the machine's response to the HF

| | Rotor angle Estimation | | Temperature Estimation | | Torque Estimation | |
|---|---|---|---|---|---|---|
| | Asymmetric | Symmetric | Asymmetric | Symmetric | Asymmetric | Symmetric |
| Resistance | ✓ [20] | × | × | ✓ [35] | × | × |
| Inductance | ✓ [7] | × | × | ✓ [37] | ✓ [24] | ✓ [27] |

✓ means "already published", × means "not published"

[1] This work was supported in part by the Research, Technological Development and Innovation Programs of the Spanish Ministry of Science and Innovation, under grant PID2019-106057RB-I00.

| Table II: HF Signal Injection Possibilities for Rotor Angle Estimation | | | | | | | | | |
|---|---|---|---|---|---|---|---|---|---|
| Injection reference frame | HF signal type (Periodic) | | | | | | | | |
| | Rotating Signal (Sinusoidal) | | Pulsating Signal (Sinusoidal) | | | | Rotating Signal (Square-Wave) | Pulsating Signal (Square-Wave) | |
| | Voltage | Current | *d*-axis | | *q*-axis | | Voltage | *d*-axis | *q*-axis |
| | | | Voltage | Current | Voltage | Current | | Voltage | Voltage |
| Stationary (*d*-axis aligned with phase A) | ✓ [7], [8] | ✓ [9] | ✓ [11] | ✗ | ✓ [11] | ✗ | ✓ [16] | ✗ | ✓ [18] |
| Synchronous (*d*-axis aligned with PM) | ✓ [10] | ✗ | ✓ [8] | ✓ [15] | ✓ [14] | ✓ [15] | ✗ | ✓ [17] | ✓ [19] |
| Used signal | Negative sequence HF current | Negative sequence HF voltage | *q*-axis HF current | *q*-axis HF voltage | *d*-axis HF current | *d*-axis HF voltage | Recons-tructed current | *q*-axis HF current | Induced HF current |
| Frequency Range | 250 – 1000 Hz | 200 – 910 Hz | 330 – 2000 Hz | 500 – 1000 Hz | 330 – 2000 Hz | 1000 Hz | 1500 Hz | 625 – 5000 Hz | 800 Hz |

reliability and increase its cost. Hence, PM temperature estimation is preferred. PM temperature estimation methods include thermal model based [32], BEMF based [33], and HF signal injection based [34]-[37] methods. Thermal models require previous knowledge of the machine geometry, materials, and cooling system. BEMF based methods do not work at standstill or low speeds. Appealing properties of HF signal injection based methods include the capability of operating in the whole speed range and the reduced sensitivity with respect to machine's geometry.

The response of the machine to the injected HF signal can be modelled as an RL load, which in a general case will consist of an average value and a differential value. The information of interest can be embedded in the resistive and/or inductive part, of either the symmetric or asymmetric components, as shown in Table I. Main facts observed from Table I are:

- Temperature estimation methods mostly rely on the symmetric behaviour of the machine, use of both inductive and resistive parts being feasible.
- Torque estimation relies on either the symmetric or asymmetric behaviour of the inductive part.
- Rotor angle estimation methods usually rely on the asymmetric part of the inductive component.

A critical aspect in the implementation of HF signal injection methods is the selection of the frequency. Generally speaking, lower frequencies will be advantageous when the information of interest is embedded in a resistive component, while higher frequencies will be preferred when the information of interest is embedded in an inductive component.

The following conclusions can be reached from the previous discussion and Table I:

- Simultaneous estimation of position, temperature, and torque, from the machine response to a HF signal seems possible.
- The fact that rotor angle estimation and temperature estimation rely on the asymmetric and symmetric parts respectively suggest that the challenges for simultaneous estimation of these two variables should be moderate.

| Table III: HF Injection Possibilities for Torque Estimation | | | | | |
|---|---|---|---|---|---|
| Injection Reference Frame | HF signal type (Periodic) | | | | |
| | Rotating Signal | Pulsating Signal | | | |
| | Voltage | Voltage | | Current | |
| | | $d$- and $q$- axis | 45º from $d$- axis | $d$- and $q$- axis | 45º from $d$- axis |
| Stationary (*d*-axis aligned with phase A) | ✓ [24] | ✗ | - | ✗ | - |
| Synchronous (*d*-axis aligned with PM) | ✓ [25] | ✗ | ✓ [26] | ✓ [27] | ✓ [28] |
| Injected signals | 1 | - | 1 | 2 | 1 |
| Used signal | Positive and negative HF current | - | *d*- and *q*-axes HF current | *d*- and *q*-axes HF voltage | *d*- and *q*-axes HF voltage |
| Estimated parameters | $L_d, L_q, \lambda_{PM}$ [24] $L_d, L_q$ [25] | - | $L_d, L_q$ | $L_d, L_q, \lambda_{PM}$ | $L_d, L_q, \lambda_{PM}$ |
| Frequency Range | 500 Hz | - | 250 Hz | 500 – 1000Hz | 500 Hz |

- means "not possible" or "no sense"

- The fact that torque estimation can be performed using either the symmetric or asymmetric parts of the machine reveals a well-known fact: load level can produce severe disturbances to both rotor angle estimation and temperature estimation methods.
- Selection of the HF signals (number of signals, signals type and frequency) will be critical to minimize the risk of interference between rotor angle, temperature and torque estimations.

This paper deals with the simultaneous estimation of rotor angle, temperature and torque in PMSM using HF signal injection. The paper is organized as follows. Section II reviews the existing literature on the estimation of these three quantities. Opportunities and challenges for simultaneous estimation are presented in Section III. Implementation of the proposed method for simultaneous estimation is presented in Section IV. Simulations results are provided in Section V. Finally, conclusions are presented in Section VI.

## II. Review of HF Signal Injection Based Rotor Angle, Temperature and Torque Estimation

In this section, the existing literature on the independent estimation of rotor angle, torque and PM temperature estimation will be reviewed.

### A. HF Signal Injection Based Rotor Angle Estimation

Rotor angle of PMSMs can be estimated by injecting a HF signal superimposed on top of the fundamental excitation [7]. Different alternatives depending on the type of HF signal and injection reference frame have been proposed, see Table II. Although all these forms of HF excitation respond to the same physical principles and can potentially provide the same performance, some differences exist in their practical implementation. Existing methods can be classified following multiple criteria: rotating vs. pulsating; sine-wave or square-wave; voltage vs. current; injection in the stationary reference frame vs, synchronous reference frame. Furthermore, pulsating HF signal injection in the synchronous reference frame allows selection of the angle of injection, e.g., $d$-axis, $q$-axis or in between $d$- and $q$-axis (45º from $d$-axis); only $d$- or $q$- axis injection has been reported for rotor angle estimation.

$$T = \frac{3}{2}\frac{P}{2}\left[\lambda_{PM} i_{qs}^{r} + \left(L_d - L_q\right) i_{ds}^{r} i_{qs}^{r}\right] \qquad (1)$$

### B. HF Signal Injection Based Torque Estimation

On-line estimation of the machine parameters involved in the general torque equation (GTE) (1), i.e., $d$- and $q$-axes inductance ($L_d$ and $L_q$) and the PM flux linkage ($\lambda_{PM}$), through HF signal injection has been recently proposed [24]-[28]. Different alternatives can be distinguished depending on the number of injected signals, magnitude (voltage or current), shape (pulsating, rotating, etc.) and injection reference frame, see Table III. Injection of a rotating voltage (whether in synchronous or stationary reference frame) or pulsating current/voltage signal at 45º from the $d$- axis allow both electromagnetic and reluctance torque estimation using a unique signal. Injection of a pulsating current in the $d$- axis of the synchronous reference frame does not allow reluctance torque estimation, as no information about the $q$- axis inductance is obtained. Hence, pulsating HF signal injection in both the $d$- and $q$-axes is required in saliency machines, e.g., IPMSMs, that produce reluctance torque. For SPMSMs, pulsating signal injection in the $d$- axis would be enough.

### C. HF Signal Injection Based PM Temperature Estimation

HF signal injection based PM temperature estimation methods rely on the variation of the stator-reflected magnet HF electrical resistance [34]-[35] or the stator $d$-axis HF inductance [37] with PM temperature. Depending on the type of HF signal and the injection reference frame, different alternatives have been proposed, see Table IV. Estimation of the $d$- axis resistance through a rotating HF voltage requires the frequency of the injected signal to be considerably higher than the fundamental one ($\omega_{HF} \gg \omega_r$); this assumption is realistic for SPMSMs but not for IPMSMs. Injection of a pulsating voltage or current signal in the $d$- axis (synchronous reference frame) allows estimation of the $d$- axis HF resistance and inductance, and therefore temperature.

## III. Combined Rotor Angle, Torque and Temperature Estimation Based on the Injection of a HF Signal

This section analyses simultaneous estimation of rotor angle, torque, and rotor temperature using HF signal injection. Table V shows the available options, using a single HF signal (first column), or two HF signals (right column). Drawbacks of injecting more than one HF signals are the increased complexity of the signal processing as well as the increased losses.

Table IV: HF Injection Possibilities for Rotor Temperature Estimation

| Injection Reference Frame | HF signal type | | | |
|---|---|---|---|---|
| | Periodic (Frequency-Based) | | | Non-Periodic (Time-Based) |
| | Rotating Signal | Pulsating Signal | | Pulse Signal |
| | Voltage | Current ($d$-axis) | Voltage ($d$-axis) | Voltage ($d$-axis) |
| Stationary ($d$-axis aligned with phase A) | ✓ [34] * | ✗ | ✗ | ✗ |
| Synchronous ($d$-axis aligned with PM) | ✗ | ✓ [35], [37] | ✓ [35] | ✓ [36] |
| Used signal | HF positive sequence current | $d$-axis HF voltage | $d$-axis HF current | $d$-axis transient current |
| Estimated parameters | $R_{dqHF}$ | $R_{dHF}$ [35] $L_{dHF}$ [37] | $R_{dHF}$ | $L_{dHF}$ |
| Frequency Range | 250 Hz | 250 – 2500 Hz | 250 Hz | - |

*Only valid for SPMSMs

| Table V: HF Injection Options for Rotor Angle, Torque and Temperature Estimation | | |
|---|---|---|
| Estimated parameter | Number of injected HF signals | |
| | Options injecting one HF signal | Options injecting two HF signals |
| Rotor angle | 1. Rotating Voltage/Current (Stationary)<br>2. Pulsating Voltage/Current ($d$- sync) | - |
| Torque | 1. Rotating Voltage (Stationary)<br>2. Rotating Voltage (Sync)<br>3. Pulsating Voltage/Current ($d$- sync) *<br>4. Pulsating Voltage/Current (45º from $d$- sync.) | 1. Pulsating Voltage/Current ($d$- sync) + Pulsating Voltage/Current ($q$- sync) |
| Magnet temperature | 1. Rotating Voltage (Stationary) *<br>2. Pulsating Voltage ($d$- sync)<br>3. Pulsating Voltage/Current ($d$- sync)<br>4. Pulsating Voltage/Current (45º from $d$- sync.) | - |
| Rotor angle and torque | 1. Rotating Voltage (Stationary)<br>2. Pulsating Voltage/Current ($d$- sync) * | 1. Pulsating Voltage/Current ($d$- sync) + Pulsating Voltage/Current ($q$- sync) |
| Rotor angle and magnet temperature | 1. Rotating Voltage (Stationary) *<br>2. Pulsating Voltage/Current ($d$- sync) | 1. Pulsating Voltage/Current ($d$- sync) + Rotating Voltage/Current (Stationary) |
| Magnet temperature and torque | 1. Rotating Voltage (Stationary) *<br>2. Pulsating Voltage/Current ($d$- sync) *<br>3. Pulsating Current (45º from $d$- sync) | 1. Pulsating Voltage/Current ($d$- sync) + Pulsating Voltage/Current ($q$- sync) |
| Rotor angle, magnet temperature and torque | 1. Rotating Voltage (Stationary) *<br>2. Pulsating Voltage/Current ($d$- sync) * | 1. Pulsating Voltage/Current ($d$- sync) + Pulsating Current ($q$- sync)<br>2. Pulsating Voltage/Current ($d$- sync) + Rotating Voltage/Current (Stationary)<br>3. Pulsating Voltage/Current (45º from $d$- sync) + Pulsating Voltage/Current ($d$- sync)<br>4. Pulsating Voltage/Current (45º from $d$- sync) + Rotating Voltage/Current (Stationary) |

*Only valid for SPMSMs

For each case, Table I shows which behaviour of the machine (symmetric/asymmetric, inductive/resistive) is to be used. Focusing on simultaneous rotor angle, torque, and magnet temperature estimation, it can be seen that the available possibilities injecting a single HF signal are limited to SPMSMs. The injection of two different HF signals opens more possibilities which are not limited to SPMSMs (i.e. can be used in any PMSM type): (i) injection of a pulsating voltage/current in the $d$-axis of the synchronous reference frame for rotor angle [8], [15] and temperature estimation [35], [37] which can be combined with a pulsating current in the $q$-axis for torque estimation [27]; (ii) injection of a rotating voltage in the stationary reference frame for rotor angle [7], [8] and torque estimation [24], which can be combined with a pulsating voltage/current in the $d$- axis for magnet temperature estimation [35], [37], (iii) injection of a pulsating HF current at 45º from the $d$-axis for temperature [35] and torque estimation [28] which can be combined with a rotating HF voltage/current in the stationary reference frame for rotor position estimation [7]-[9] and (iv) injection of a pulsating voltage/current in the $d$-axis of the synchronous reference frame for rotor angle estimation [8], [15] which can be combined with

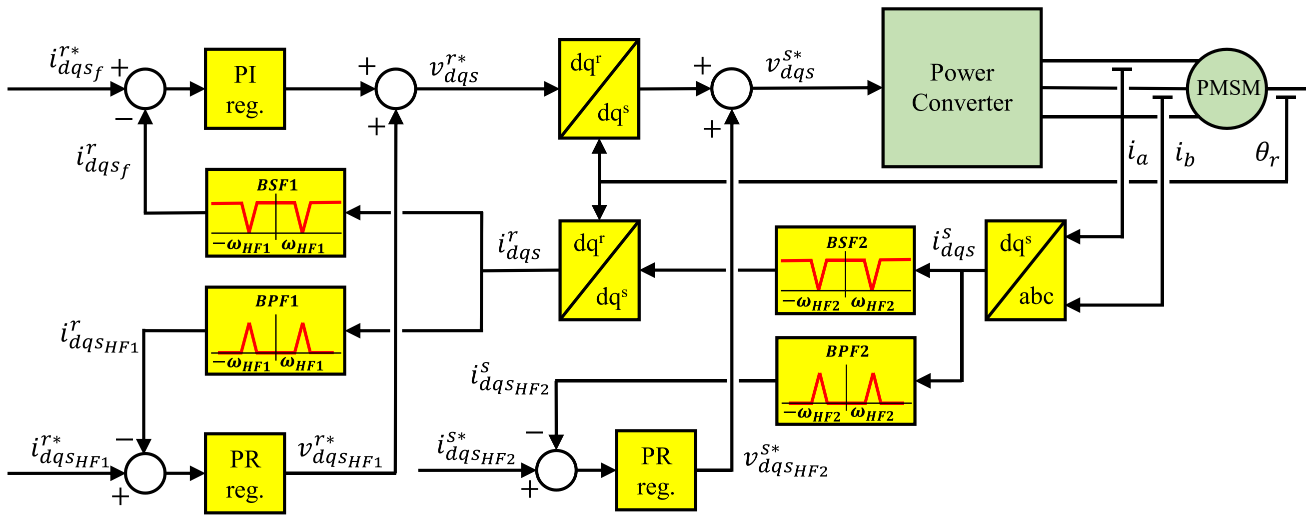

Fig. 1: Control scheme for simultaneous rotor angle, torque and magnet temperature estimation combining a pulsating HF current 45ºshifted from the $d$-axis ($HF_1$) and a rotating HF current in the stationary reference frame ($HF_2$).

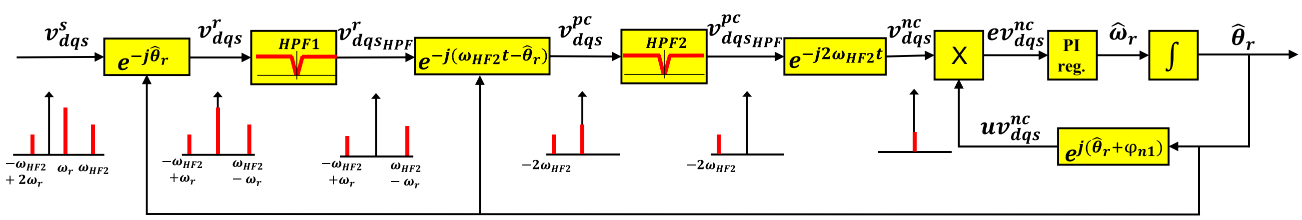

Fig. 2: Rotor position estimation control block diagram (PLL).

the same signals as in (iii) for torque and magnet temperature estimation.

Following the preceding discussion, the combined use of a pulsating HF current 45º shifted from the *d*-axis and a rotating HF current in the stationary reference frame has been chosen. This option is advantageous in terms of injection frequency selection: lower frequencies will be used for the pulsating current as it is preferable for $dq$ -axes resistance, $R_{dq_{HF}}$ (for magnet temperature estimation) and inductance, $L_{dq_{HF}}$ (for torque estimation) estimation, while higher frequencies for the rotating HF current are preferable for rotor angle estimation. In addition, it can be observed that this option does not require to combine parameters estimated with different HF signals, i.e., both rotor angle, torque as well as magnet temperature are independently estimated through a single HF signal.

## IV. Implementation

This section discusses the implementation of the selected method. Fig. 1 shows the corresponding block diagram. A pulsating HF current 45º shifted from the *d*-axis ($HF_1$) and a rotating HF current in the stationary reference frame ($HF_2$) are injected. Two band-stop filters (BSF1 and BSF2) are used to remove both HF components ( $\omega_{HF1}$ and $\omega_{HF2}$ ) in the fundamental current feedback. Proportional resonant (PR) controllers are used to control the injected HF currents, band-pass filters (BPF1 and BPF2) being used to isolate each HF component in the corresponding HF current feedback, i.e., $\omega_{HF1}$ for the pulsating HF current feedback, and $\omega_{HF2}$ for the rotating HF current feedback.

### A. Rotor Angle Estimation Using Rotating HF Current Injection in the Stationary Reference Frame

If a sinusoidal rotary HF current signal (2) is injected into the stator terminals of a PMSM, the resulting HF voltages are represented by (3) assuming a pure inductive behaviour of the PMSM, where $\sum L_s$ (4) and $\Delta L_s$ (5) are the mean and differential inductances respectively. (3) can be also expressed as (6), where $V_{pc}$ (7) is the magnitude of the positive sequence component and $V_{nc}$ (8) the magnitude of the negative sequence component. It can be observed from (6) that the resulting stator HF voltage can be decomposed into a positive sequence component, that does not provide any information about the rotor position, and a negative sequence component, with rotor position information [7].

$$i^s_{dqs_{HF2}} = I_{HF2}\begin{bmatrix}\cos(\omega_{HF2}t)\\ \sin(\omega_{HF2}t)\end{bmatrix} \tag{2}$$

$$v^s_{dqs_{HF2}} = j\omega_{HF2} i^s_{dqs_{HF2}} \cdot \\ \cdot\begin{bmatrix}\sum L_s + \Delta L_s\cos(2\theta_r) & -\Delta L_s \sin(2\theta_r)\\ -\Delta L_s\sin(2\theta_r) & \sum L_s - \Delta L_s\cos(2\theta_r)\end{bmatrix} \tag{3}$$

$$\sum L_s = \frac{L_{ds}+L_{qs}}{2} \quad (4) \qquad \Delta L_s = \frac{L_{qs}-L_{ds}}{2} \quad (5)$$

$$v^s_{dqs\,HF2} = v^r_{dqs\,HF2pc} + v^r_{dqs\,HF2nc} = jV_{pc}e^{j\omega_{HF2}} + \\ +V_{nc}e^{-j(\omega_{HF2}t-2\theta_r)} \tag{6}$$

$$V_{pc} = \omega_{HF2} I_{HF2} \sum L_s \quad (7) \qquad V_{nc} = \omega_{HF2} I_{HF2} \Delta L \quad (8)$$

Fig. 2 shows the control block diagram for rotor position estimation when using a rotating HF current injection. The input of the control block diagram is the stator voltage in the stator reference frame, $v^s_{dqs}$ which is first transformed to a reference frame synchronous with the estimated rotor position, $v^r_{dqs}$.

Two high-pass filters (HPF) are used to remove the fundamental voltage (HPF1), $v^r_{dqs_{HPF}}$ being obtained, and the positive sequence of the HF voltage (HPF2), $v^{pc}_{dqs_{HPF}}$ being obtained; the resulting voltage consisting therefore only of the negative sequence component, see $v^{nc}_{dqs}$. $v^{nc}_{dqs}$ will feed a PLL used to estimate the rotor position [9].

### B. Torque and Temperature Estimation through Pulsating HF Signal Injection at 45º from the d-axis

Simultaneous rotor temperature, $T_r$ and torque, $T$ estimation can be achieved through the injection of a pulsating HF signal at 45º from the *d*-axis. A resonant controller can be used to inject the HF current, $i^{r*}_{dqs_{HF1}}$ (9), the HF voltage, $v^{r*}_{dqs_{HF1}}$, (10) being thus commanded. Estimation of the $d$- axis HF resistance, $R_{d_{HF1}}$, and inductance, $L_{d_{HF1}}$, can be done through the measured $d$-axis HF current, $i^{r'}_{dqs_{HF1}}$, (11), and the commanded $d$- axis HF voltage, $v^{r'}_{dqs_{HF1}}$, (12). Both (11) and (12) can be decomposed into a positive ($i^{r'}_{dqs_{HF_{pc}1}}$ and $v^{r'}_{dqs_{HF1_{pc}}}$) and negative sequence component ($i^{r}_{dqs_{HF1_{nc}}}$ and $v^{r}_{dqs_{HF1_{nc}}}$), see (13) and (14). The $d$- axis HF impedance, $Z_d$ can be obtained either from the positive or the negative sequence component, as shown in (15). Taking the real part of (15) the $d$- axis HF resistance, $R_{d_{HF1}}$ is obtained (16). Taking the imaginary part of (15) the $d$- axis HF inductance, $L_{d_{HF1}}$ is obtained (17). Following an analogous process, but using the $q$-axis voltage and current (18)-(22), the $q$-axis HF inductance, $L_{q_{HF1}}$ can be also obtained (23).

$$i^{r*}_{dqs_{HF1}} = \begin{bmatrix}\bar{I}^{r*}_{ds\,HF1}\\ \bar{I}^{r*}_{qs\,HF1}\end{bmatrix} = \begin{bmatrix}I^*_{HF1}\cos(\omega_{HF1}t)\\ I^*_{HF1}\cos(\omega_{HF1}t)\end{bmatrix} \tag{9}$$

$$v^{r*}_{dqs_{HF1}} = \begin{bmatrix}\bar{V}^{r*}_{ds\,HF1}\\ \bar{V}^{r*}_{qs\,HF1}\end{bmatrix} \\ = \begin{bmatrix}(R_{d_{HF1}} + j\omega_{HF1}L_{d_{HF1}})\bar{I}^r_{ds\,HF1} - \omega_r L_{q_{HF1}}\bar{I}^r_{qs\,HF1}\\ (R_{q_{HF1}} + j\omega_{HF1}L_{q_{HF1}})\bar{I}^r_{qs\,HF1} + \omega_r L_{d_{HF1}}\bar{I}^r_{ds\,HF1}\end{bmatrix} \tag{10}$$

$$i^{r\prime}_{dqs_{HF1}} = \begin{bmatrix}\bar{I}^{r*}_{ds\,HF1}\\ 0\end{bmatrix} = \begin{bmatrix}I^*_{HF1}\cos(\omega_{HF1}t)\\ 0\end{bmatrix} \tag{11}$$

$$v^{r\prime}_{dqs_{HF1}} \\ = \begin{bmatrix}(R_{d_{HF1}} + j\omega_{HF1}L_{d_{HF1}})\bar{I}^r_{ds\,HF1} - \omega_r L_{q_{HF1}}\bar{I}^r_{qs\,HF1}\\ 0\end{bmatrix} \tag{12}$$

$$i^{r'}_{dqs_{HF1}} = \frac{\left|i^{r'}_{dqs_{HF1}}\right|}{2} e^{j\omega_{HF1}t} + \frac{\left|i^{r'}_{dqs_{HF1}}\right|}{2} e^{-j\omega_{HF1}t} = = i^{r'}_{dqs_{HF1pc}} + i^{r'}_{dqs_{HF1nc}} \tag{13}$$

$$v^{r'}_{dqs_{HF1}} = \frac{\left|v^{r'}_{dqs_{HF1}}\right|}{2} e^{j(\omega_{HF1}t-\varphi_{Z_d})} + \frac{\left|v^{r'}_{dqs_{HF1}}\right|}{2} e^{j(-\omega_{HF1}t+\varphi_{Z_d})} = v^{r'}_{dqs_{HF1pc}} + v^{r'}_{dqs_{HF1nc}} \tag{14}$$

$$Z_d = R_{d_{HF1}} - \omega_r L_{q_{HF1}} + j\omega_{HF1} L_{d_{HF1}} = = \frac{v^{r'}_{dqs_{HF1pc}}}{i^{r'}_{dqs_{HF1pc}}} = \frac{v^{r'}_{dqs_{HF1nc}}}{i^{r'}_{dqs_{HF1nc}}} \tag{15}$$

$$R_{d_{HF1}} = \Re\left[Z_{d_{HF1}}\right]/\omega_{HF1} \tag{16}$$

$$L_{d_{HF1}} = \Im\left[Z_{d_{HF1}}\right]/\omega_{HF1} \tag{17}$$

$$i^{r''}_{dqs_{HF1}} = \begin{bmatrix} 0 \\ \bar{I}^{*}_{qs_{HF1}} \end{bmatrix} = \begin{bmatrix} 0 \\ I_{HF1}\cos\left(\omega_{HF1}t\right) \end{bmatrix} \tag{18}$$

$$v^{r''}_{dqs_{HF1}} = \begin{bmatrix} 0 \\ \left(R_{q_{HF1}} + j\omega_{HF1} L_{q_{HF1}}\right) \bar{I}^{r}_{qs_{HF1}} + \omega_r L_{d_{HF1}} \bar{I}^{r}_{ds_{HF1}} \end{bmatrix} \tag{19}$$

$$i^{r*}_{dqs_{HF1}} = \frac{\left|i^{r''}_{dqs_{HF1}}\right|}{2} e^{j\omega_{HF1}t} + \frac{\left|i^{r''}_{dqs_{HF1}}\right|}{2} e^{-j\omega_{HF1}t} = i^{r''}_{dqs_{HF1pc}} + i^{r''}_{dqs_{HF1nc}} \tag{20}$$

$$v^{r''}_{dqs_{HF1}} = \frac{\left|v^{r''}_{dqs_{HF1}}\right|}{2} e^{j(\omega_{HF1}t-\varphi_{Z_d})} + \frac{\left|v^{r''}_{dqs_{HF1}}\right|}{2} e^{j(-\omega_{HF1}t+\varphi_{Z_d})} = v^{r''}_{dqs_{HF1pc}} + v^{r''}_{dqs_{HF1nc}} \tag{21}$$

$$Z_q = R_{q_{HF1}} - \omega_r L_{d_{HF1}} + j\omega_{HF1} L_{q_{HF1}} = \frac{v^{r''}_{dqs_{HF1pc}}}{i^{r''}_{dqs_{HF1pc}}} = \frac{v^{r''}_{dqs_{HF1nc}}}{i^{r''}_{dqs_{HF1nc}}} \tag{22}$$

$$L_{q_{HF1}} = \Im\left[Z_{q_{HF1}}\right]/\omega_{HF1} \tag{23}$$

According to [27], $\lambda_{PM}$ variation with the $d$- axis inductance is given by (24) where $\lambda_{PM0}$ and $L_{d0}$ are the PM flux and $d$- axis inductance at the room temperature ($T_{r0}$) and when no $dq$-axis fundamental current is injected respectively, $L_{d_{HF1}}$ is the $d$- axis inductance when the magnet temperature is $T_r$ and when $dq$-axis fundamental current is injected (17) and $K_{BEMF}$ is the coefficient linking the $d$- axis HF inductance with the PM flux.

$$\lambda_{PM} = \left(\lambda_{PM0} + k_{BEMF}\frac{L_{d_{HF1}} - L_{d0}}{L_{d0}}\right) \tag{24}$$

Then, substituting (17), (23) and (24) in the GTE (1), the output torque, $T$, can be finally estimated.

PM temperature can be estimated through $d$- axis HF resistance (25) [35], being $T_s$ and $T_r$ the stator and rotor temperatures respectively, $T_0$ the room temperature, $R_{ds_{HF1}}$ and $R_{dr_{HF1}}$ the stator and rotor contributions to the $d$- axis HF resistance, and $\alpha_{cu}$ and $\alpha_{mag}$ the copper and magnet thermal resistive coefficients respectively.

$$R_{d_{HF1(T_s,T_r)}} = R_{ds_{HF1(T_s)}} + R_{dr_{HF1(T_r)}} = = R_{ds_{HF1(T_0)}}\left(1 + \alpha_{cu}(T_s - T_0)\right) + R_{dr_{HF1(T_0)}}\left(1 + \alpha_{mag}(T_r - T_0)\right) \tag{25}$$

Fig. 3 shows the signal processing block diagram for simultaneous torque estimation (GTE) and rotor temperature estimation ($d$- axis HF resistance).

## V. Simulation Results

This section presents simulation results showing simultaneous rotor angle, torque, and temperature estimation. Rotor temperature is assumed to increase proportionally to the squared stator current due to joule losses; an unrealistically low value of the thermal constant has been used to reduce the simulation time. It is noted that

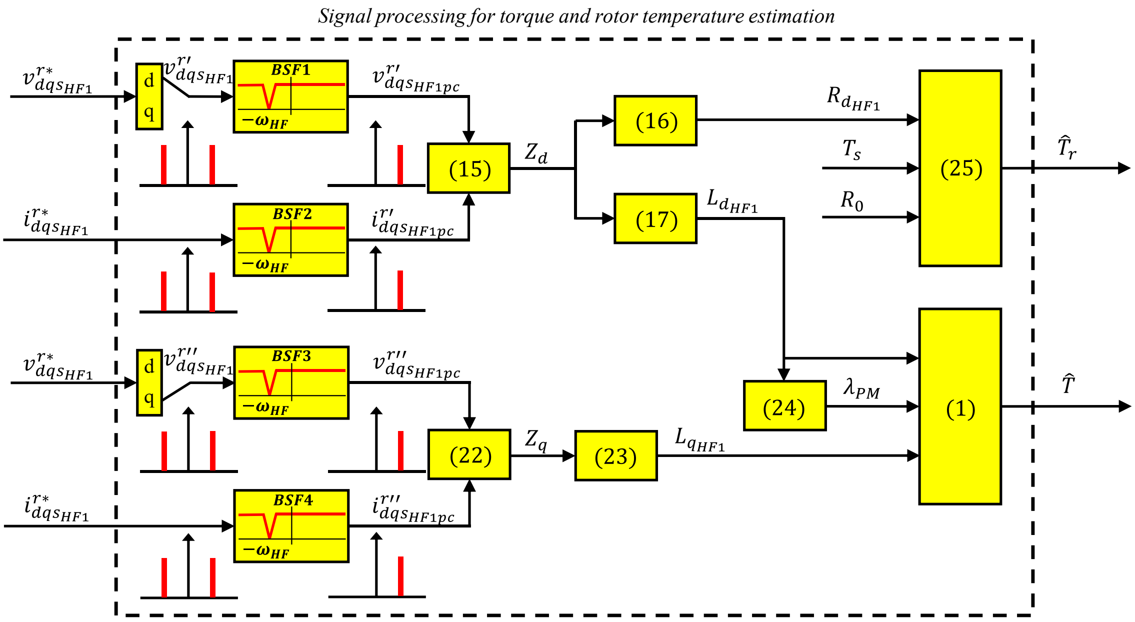


Fig. 3: Torque and rotor temperature estimation control block diagram.

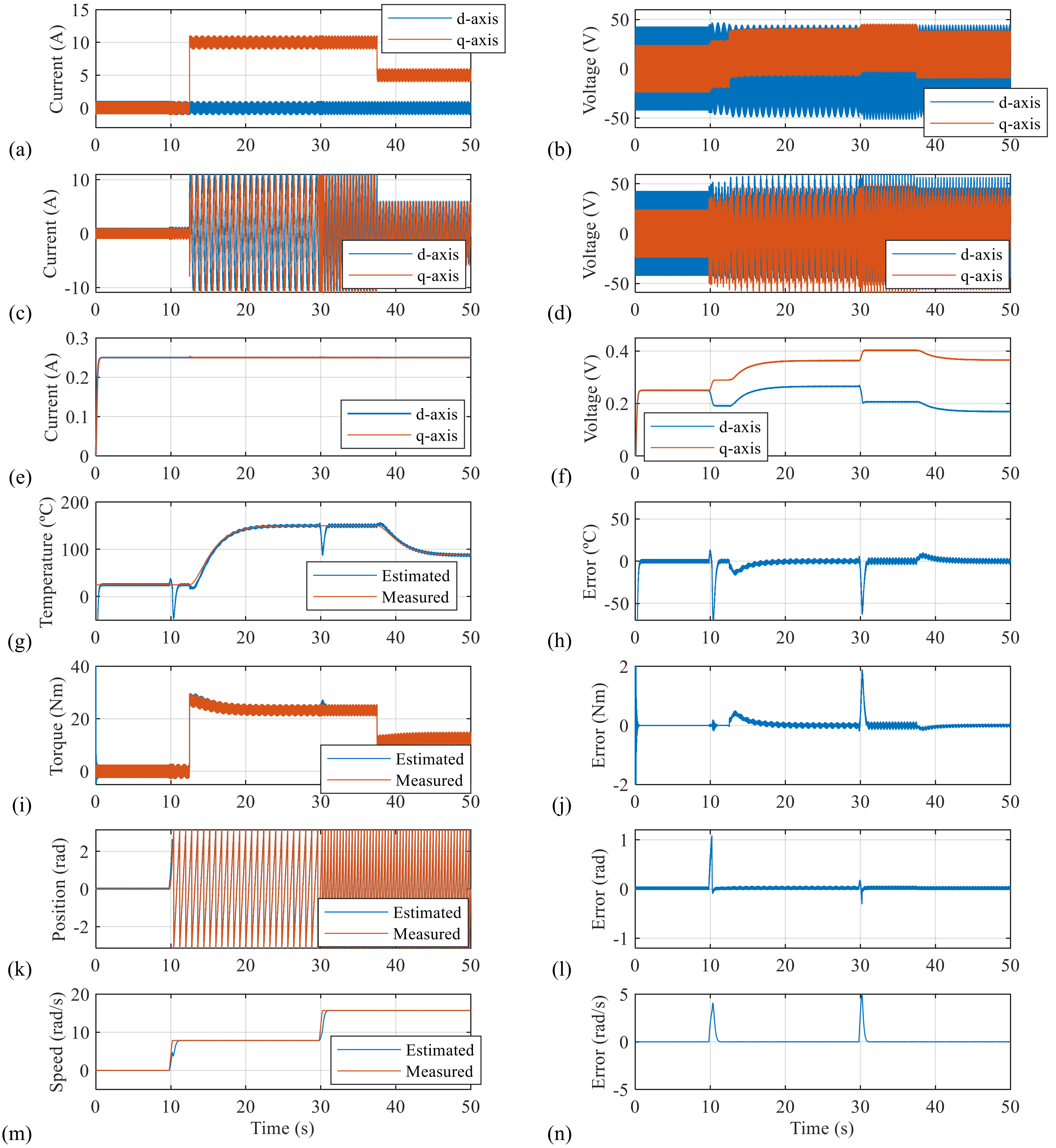


Fig. 4: (a) *dq*-axes current and (b) voltage in the synchronous reference frame, (c) *dq*-axes current and (d) voltage in the stationary reference frame, (e) pulsating HF current ($HF_1$), (f) resulting stator HF voltage, (g) measured and estimated temperature, (h) temperature estimation error, (i) measured and estimated torque, (j) torque estimation error, (k) measured and estimated rotor angle, (l) rotor angle estimation error, (m) measured and estimated speed and (n) speed estimation error. $\omega_{HF1}$=2·π·250 rad/s, $I_{HF1}$=0.05pu, $\omega_{HF2}$=2·π·500 rad/s and $I_{HF2}$=0.05pu.

this has no further effects on the results. Fig. 4 (a) and (b) show the *dq*- axes currents and voltages in the synchronous reference frame respectively, (c) and (d) show the *dq*- axes currents and voltages in the stationary reference frame, (e) shows the injected pulsating HF current ($HF_1$), (f) shows the resulting stator HF voltage, (g) and (h) show both the measured and estimated temperature and the corresponding temperature estimation error, (i) and (j) show both the measured and estimated torque and the corresponding torque error, (k) and (l) show both the measured and estimated rotor position and the resulting rotor position estimation error, finally (m) and (n) show the measured and estimated speed and the resulting speed estimation error. Steady state estimation errors are seen to be <5ºC for magnet temperature (Fig. 4h), <0.12 Nm (0.4%) for torque (Fig. 4j) and < 0.07 rad (Fig. 4l) for rotor angle, respectively.

## VI. Conclusions

This paper proposes the use of HF signal injection for simultaneous rotor angle, torque, and magnet temperature estimation in PMSMs. Available options in terms of number and types of signals that could be injected have been discussed. Simultaneous rotor angle, torque and magnet temperature estimation using a single HF signal has been shown to be only feasible for SPMSMs, the use of at least two HF signals being required for IPMSMs.

Combination of a rotating HF current in the stationary reference frame (rotor angle estimation) and a pulsating HF current in the synchronous reference frame (torque and magnet temperature estimation) has been chosen as the preferred solution. Simulation results have been provided to demonstrate the viability of the proposed method. Experimental verification of the proposed method is ongoing.

## REFERENCES


[1] Maxonmotorusa.com, "maxon sensor - Key information," Sep. 20, 2020. [Online]. Available: http://www.maxonmotorusa.com/

[2] Figueiredo, "Resolver models for manufacturing," IEEE Trans. Ind. Electron., 58(8): 3693–3700, Aug. 2011

[3] R. M. Kennel and S. Basler, "New developments in capacitive encoders for servo drives," 2008 International Symposium on Power Electronics, Electrical Drives, Automation and Motion, Ischia, 2008, pp. 190-195, doi: 10.1109/SPEEDHAM.2008.4581311.

[4] B. S. Nauduri and G. Shaga, "A novel approach of using a planar inductive position sensor for the Permanent magnet synchronous motor control application," 2018 IEEE Sensors Applications Symposium (SAS), Seoul, 2018, pp. 1-5, doi: 10.1109/SAS.2018.8336708.

[5] P. Kejik, S. Reymond, and R. S. Popovic, "Purely CMOS angular position sensor based on a new Hall microchip," in Proc. 34th Annu. Conf. IEEE Ind. Electron., Nov. 10–13, 2008, pp. 1777–1781.

[6] L. A. de S. Ribeiro, M. C. Harke, and R. D. Lorenz, "Dynamic properties of back-EMF based sensorless drives," in Conf. Rec. IEEE IAS Meeting, Oct. 2006, vol. 4, pp. 2026–2033

[7] M. W. Degner and R. D. Lorenz, "Using multiple saliencies for the estimation of flux, position, and velocity in AC machines," in IEEE Transactions on Industry Applications, vol. 34, no. 5, pp. 1097-1104, Sept.-Oct. 1998, doi: 10.1109/28.720450.

[8] Y. Jeong, R. D. Lorenz, T. M. Jahns, and S.-K. Sul, "Initial rotor position estimation of an interior permanent-magnet synchronous machine using carrier-frequency injection methods," IEEE Trans. Ind. Appl., vol. 41, no. 1, pp. 38–45, Jan./Feb. 2005.

[9] L.A.S. Ribeiro, M.W. Degner, F. Briz y R.D. Lorenz. Comparison of carrier signal voltage and current injection for the estimation of flux angle or rotor position. En IEEE Industry Applications Society Annual Meeting. IAS'98, tomo 1, páginas 452–459. St. Louis, MO, USA, 1998.

[10] C. Caruana, G. M. Asher, K. J. Bradley and M. Woolfson, "Flux position estimation in cage induction machines using synchronous HF injection and Kalman filtering," in IEEE Transactions on Industry Applications, vol. 39, no. 5, pp. 1372-1378, Sept.-Oct. 2003, doi:

[11] J. M. Liu and Z. Q. Zhu, "Novel Sensorless Control Strategy With Injection of High-Frequency Pulsating Carrier Signal Into Stationary Reference Frame," in IEEE Transactions on Industry Applications, vol. 50, no. 4, pp. 2574-2583, July-Aug. 2014, doi: 10.1109/TIA.2013.2293000.

[12] M. Linke, R. Kennel, and J. Holtz, "Sensorless speed and position control of synchronous machines using alternating carrier injection," in Proc. IEEE IEMDC, 2003, vol. 2, pp. 1211–1217.

[13] G. Foo and M. F. Rahman, "Sensorless Sliding-Mode MTPA Control of an IPM Synchronous Motor Drive Using a Sliding-Mode Observer and HF Signal Injection," in IEEE Transactions on Industrial Electronics, vol. 57, no. 4, pp. 1270-1278, April 2010, doi: 10.1109/TIE.2009.2030820

[14] M. J. Corley and R. D. Lorenz, "Rotor position and velocity estimation for a salient-pole permanent magnet synchronous machine at standstill and high speed," IEEE Trans. Ind. Appl., vol. 34, no. 4, pp. 784–789, Jul./Aug. 1998

[15] M. Seilmeier, A. Boehm, I. Hahn and B. Piepenbreier, "Identification of time-variant high frequency parameters for sensorless control of PMSM using an internal model principle based high frequency current control," 2012, 20th International Conference on Electrical Machines, Marseille, 2012, pp. 987-993, doi: 10.1109/ICElMach.2012.6349996.

[16] G. Wang, D. Xiao, G. Zhang, C. Li, X. Zhang and D. Xu, "Sensorless Control Scheme of IPMSMs Using HF Orthogonal Square-Wave Voltage Injection Into a Stationary Reference Frame," in IEEE Transactions on Power Electronics, vol. 34, no. 3, pp. 2573-2584, March 2019, doi: 10.1109/TPEL.2018.2844347.

[17] S. Yang, "Saliency-Based Position Estimation of Permanent-Magnet Synchronous Machines Using Square-Wave Voltage Injection With a Single Current Sensor," in IEEE Transactions on Industry Applications, vol. 51, no. 2, pp. 1561-1571, March-April 2015, doi: 10.1109/TIA.2014.2358796.

[18] J. Zhao, S. Nalakath and A. Emadi, "A High Frequency Injection Technique With Modified Current Reconstruction for Low-Speed Sensorless Control of IPMSMs With a Single DC-Link Current Sensor," in IEEE Access, vol. 7, pp. 136137-136147, 2019, doi: 10.1109/ACCESS.2019.2942148.

[19] Y. Yoon and S. Sul, "Sensorless Control for Induction Machines Based on Square-Wave Voltage Injection," in IEEE Transactions on Power Electronics, vol. 29, no. 7, pp. 3637-3645, July 2014, doi: 10.1109/TPEL.2013.2278103.

[20] P. García, F. Briz, D. Reigosa, C. Blanco and J. M. Guerrero, "On the use of high frequency inductance vs. high frequency resistance for sensorless control of AC machines," *2011 Symposium on Sensorless Control for Electrical Drives*, Birmingham, 2011, pp. 90-95, doi: 10.1109/SLED.2011.6051550.

[21] C. Lin, S. Liang, J. Chen, and X. Gao, "A Multi-Objective Optimal Torque Distribution Strategy for Four In-Wheel-Motor Drive Electric Vehicles", IEEE Access, 7: 64627–64640, 2019.

[22] [Online]. Available: http://www.interfacetorque.co.uk. Accessed on: Sep. 20, 2020.

[23] P. Sue, D. Wilson, L. Farr, and A. Kretschmar, "High precision torque measurement on a rotating load coupling for power generation operations", in IEEE Int. Instrum. Meas. Technol. Conf. Proc., pp: 518– 523, May 2012.

[24] W. Xu and R. D. Lorenz, "High-Frequency Injection-Based Stator Flux Linkage and Torque Estimation for DB-DTFC Implementation on IPMSMs Considering Cross-Saturation Effects," in IEEE Transactions on Industry Applications, vol. 50, no. 6, pp. 3805-3815, Nov.-Dec. 2014, doi: 10.1109/TIA.2014.2322134.

[25] M. Martinez, D. F. Laborda, D. Reigosa, D. Fernández, J. M. Guerrero and F. Briz, "SynRM Sensorless Torque Estimation Using High Frequency Signal Injection," 2019 IEEE 10th International Symposium on Sensorless Control for Electrical Drives (SLED), Turin, Italy, 2019, pp. 1-5, doi: 10.1109/SLED.2019.8896220.

[26] D. Reigosa, Y. g. Kang, M. Martínez, D. Fernández, J. M. Guerrero and F. Briz, "SPMSMs Sensorless Torque Estimation Using High-Frequency Signal Injection," in IEEE Transactions on Industry Applications, vol. 56, no. 3, pp. 2700-2708, May-June 2020, doi: 10.1109/TIA.2020.2975757.

[27] M. Martinez, D. Reigosa, D. Fernández, J. M. Guerrero, and F. Briz, "PMSMs Torque Estimation Using Pulsating HF Current Injection", in 2018 IEEE 9th Int. Symp. Sensorless Control Electr. Drives SLED, pp: 96–101, Sep. 2018.

[28] D. F. Laborda, D. Díaz Reigosa, D. Fernández, K. Sasaki, T. Kato and F. Briz, "Enhanced Torque Estimation in Variable Leakage Flux PMSM Combining High and Low Frequency Signal Injection," *2020 IEEE Energy Conversion Congress and Exposition (ECCE)*, Detroit, MI, USA, 2020, pp. 1764-1771, doi: 10.1109/ECCE44975.2020.9235869

[29] F. Jukic, D. Sumina, and I. Erceg, "Comparison of torque estimation methods for interior permanent magnet wind power generator", in Int. Conf. Electr. Drives Power Electron. EDPE, pp: 291–296, Oct. 2017.

[30] Z. Lin, D. S. Reay, B. W. Williams, and X. He, "Online Modeling for Switched Reluctance Motors Using B-Spline Neural Networks", IEEE Trans. Ind. Electron., 54(6): 3317–3322, Dec. 2007.

[31] Miguel A. Perez. Instrumntación electrónica, volume 1 of 1. Paraninfo, The address, 1 edition, 1 2014. Spanish.

[32] M. Kamiya, Y. Kawase, Y. Kosada, and N. Matsui, "Temperature distribution analysis of permanent magnet in interior permanent magnet synchronous motor considering PWM carrier harmonics," in Proc. IEEEICEMS, Oct. 2007, pp. 2023–2027.

[33] K. Liu and Z. Q. Zhu, "Online estimation of the rotor flux linkage and voltage source inverter nonlinearity in permanent magnet synchronous machine drives," *IEEE Trans. Power. Electron.*, vol. 29, no. 1, pp. 418–427, Jan. 2014.

[34] D. Reigosa, F. Briz, P. García, J. M. Guerrero, and M.W. Degner, "Magnet temperature estimation in surface PM machines using high frequency signal injection," IEEE Trans. Ind. Appl., vol. 46, no. 4, pp. 1468–1475, Jul./Aug. 2010.

[35] D. Reigosa, D. Fernandez, H. Yoshida, T. Kato, and F. Briz, "Permanent magnet temperature estimation in PMSMs using pulsating high frequency current injection," IEEE Trans. Ind. Appl., vol. 51, no. 4, pp. 3159–3168, Jul./Aug. 2015.

[36] M Ganchev, C. Kral, and T. Wolbank, "Compensation of speed dependency in sensorless rotor temperature estimation for permanent-magnet synchronous motors," IEEE Trans. Ind. Appl., vol. 49, no. 6, pp. 2487–2495, Nov./Dec. 2013.

[37] D. Reigosa, D. Fernández, M. Martínez, J. M. Guerrero, A. B. Diez and F. Briz, "Magnet Temperature Estimation in Permanent Magnet Synchronous Machines Using the High Frequency Inductance," in IEEE Transactions on Industry Applications, vol. 55, no. 3, pp. 2750-2757, May-June 2019, doi: 10.1109/TIA.2019.2895557.